UC Santa Barbara
UC Santa Barbara Previously Published Works

Title

Strong Adhesion and Cohesion of Chitosan in Aqueous Solutions

Authors

Lee, Dong Woog
Lim, Chanoong
Israelachvili, Jacob N
et al.

Peer reviewed

Strong Adhesion and Cohesion of Chitosan in Aqueous Solutions

Dong Woog Lee,[†] Chanoong Lim,[‡] Jacob N. Israelachvili,*[,†,§] and Dong Soo Hwang*[,‡,⊥,¶,△]

[†]Department of Chemical Engineering, University of California at Santa Barbara, CA 93106, United States

[‡]School of Interdisciplinary Bioscience and Bioengineering, Pohang University of Science and Technology (POSTECH), Pohang 790-784, South Korea

[§]Materials Department, University of California at Santa Barbara, CA 93106, United States

[⊥]School of Environmental Science and Engineering, [¶]POSTECH Ocean Science and Technology Institute (POSTI), [△]Integrative Biosciences and Biotechnology, Pohang University of Science and Technology (POSTECH), Pohang 790-784, South Korea

Ⓢ *Supporting Information*
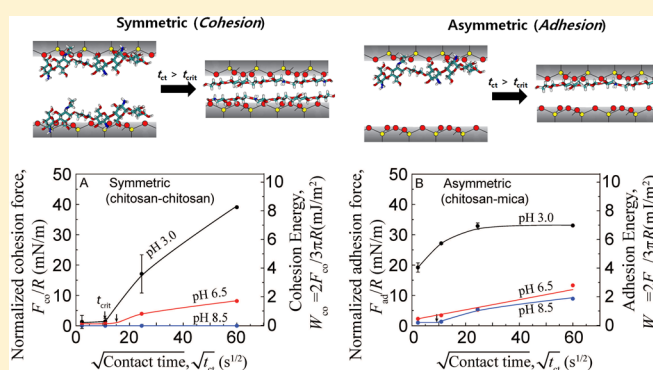
ABSTRACT: Chitosan, a load-bearing biomacromolecule found in the exoskeletons of crustaceans and insects, is a promising biopolymer for the replacement of synthetic plastic compounds. Here, surface interactions mediated by chitosan in aqueous solutions, including the effects of pH and contact time, were investigated using a surface forces apparatus (SFA). Chitosan films showed an adhesion to mica for all tested pH ranges (3.0–8.5), achieving a maximum value at pH 3.0 after a contact time of 1 h ($W_{ad} \sim 6.4$ mJ/m^2). We also found weak or no cohesion between two opposing chitosan layers on mica in aqueous buffer until the critical contact time for maximum adhesion (chitosan–mica) was reached. Strong cohesion ($W_{co} \sim 8.5$ mJ/m^2) between the films was measured with increasing contact times up to 1 h at pH 3.0, which is equivalent to ~60% of the strongest, previously reported, mussel underwater adhesion. Such time-dependent adhesion properties are most likely related to molecular or molecular group reorientations and interdigitations. At high pH (8.5), the solubility of chitosan changes drastically, causing the chitosan–chitosan (cohesion) interaction to be repulsive at all separation distances and contact times. The strong contact time and pH-dependent chitosan–chitosan cohesion and adhesion properties provide new insight into the development of chitosan-based load-bearing materials.

■ INTRODUCTION

Chitin, the major structural component in the exoskeletons of crustaceans and insects, is the second most abundant natural biopolymer after cellulose.[1−4] However, its application is limited as chitin is a biopolymer that is not soluble in water or other common organic solvents. For this reason, chitin is generally converted to its partially deacetylated derivative, chitosan, which is soluble in dilute acidic medium.[2,5] Chitin and chitosan compose a family of linear structural polysaccharides that consist of varying amounts of *N*-acetyl-D-glucosamine and D-glucosamine units connected by *β*-1,4 linkages (Figure 1). The degree of acetylation (DA) which represents a percentage of *N*-acetyl-D-glucosamine unit with respect to the total number of the two units defines the two terms, chitin and chitosan, and affects their solubility in dilute acidic medium (2 < pH < 6). Conventionally, the DA value of chitosan is usually considered

to be below 50%, while chitosan is soluble in dilute acidic buffer. However, a specific DA to characterize chitin versus chitosan has not yet been determined.[6]

Chitosan is one of the most widely used biopolymers for numerous applications in various fields such as fabrics,[3] cosmetics,[7] water treatment,[8] and food processing[9] because of its ability to bind to a variety of natural or synthetic molecules such as nanoparticles, drugs, polymers, metal ions, and cells. Accordingly, formulations of chitosan with such molecules have been prepared in a wide range of forms including films, hydrogels, fibers, and emulsions and have been utilized in numerous fields.[9] Moreover, chitosan is also a highly attractive
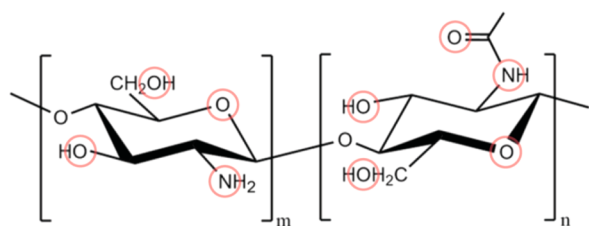
Figure 1. Chemical structures of chitin and chitosan. Chitin and chitosan are random copolymers of D-glucosamine (m) and N-acetyl-D-glucosamine (n) unit (chitin n > m; chitosan m > n). Red circles indicate the hydrogen-bonding sites.

biomaterial in the medical and pharmaceutical fields because of its low toxicity and biodegradability as well as in wound healing and antimicrobial activity.[10]

In spite of these many applications of chitosan, there have been few systematic studies conducted with regard to the interaction between chitosan with other substrates and itself. Chitosan can form fibrous self-assembled structures based on hydrogen-bond networks in aqueous solutions, and conformational variations of the chitosan assembly have been reported[11] to depend on local environment changes around chitosan (e.g., pH, temperature, types of salt, and types of acids).[12−18] Therefore, understanding the interactions of chitosan under different aqueous buffer conditions is useful for the interpretation and application of chitin/chitosan based biological materials. Only Claesson and Ninham measured pH-dependent interaction forces between adsorbed chitosan layers by a surface forces apparatus (SFA),[19] an instrument that has been widely used to measure the intermolecular forces in various biological systems[20−23] with nano-Newton force sensitivity and angstrom distance resolution.[24] These authors measured rather small adhesion forces of chitosan to mica or chitosan itself ($W_{co} \sim 0.5$ mJ/m^2). This behavior is not inconsistent with semicrystalline phase formation of chitosan fibers depending on the degree of deacetylations. In addition, chitosan has reactive primary amine groups with a hydrophilic helical structure, which help to form various intermolecular and intramolecular interactions. Therefore, we hypothesize that longer contact times during the force measurement compared to the previous study might enhance cohesion/adhesion between two opposing chitosan layers or between a chitosan layer and mica.

Here, unlike in the previous SFA study, the effects of contact time on chitosan interactions in aqueous solutions were investigated using an SFA because longer contact times can induce molecular reorientations and interdigitations that can significantly increase adhesion and cohesion.[25] Our results suggest that the contact time plays a critical role in the strong cohesion between chitosan films, which is likely due to molecular reorientations and interdigitations of the chitosan film during prolonged contact times.

■ MATERIALS AND METHODS

Materials. Chitosan (MW 120 000−150 000) was purchased from Sigma-Aldrich. The solubility of chitosan was ∼80 mg/mL in 150 mM acetic acid at 25 °C, and the chitosan was only soluble in acetate buffer solutions of pH below 6.5 The degree of acetylation (DA) of chitosan was determined by ^{1}H NMR.[26] For the ^{1}H NMR measurement, chitosan was suspended in DCl and was acquired with 16 transients, with an acquisition time of 3.642 s, and with a delay of 1.500 s. The

temperature was controlled at 70 °C to increase chitosan solubility. The degree of acetylation of chitosan was calculated from the areas of the signals in 2.1 ppm (methyl) and from the sum of the areas from 3.2 to 4.2 ppm (H2, H3, H4, H5, H6, and H6) in the ^{1}H NMR according to eq 1.

$$\%DA = \left(\frac{2A_{CH_3}}{A_{H2-H6}} \right) \times 100 \tag{1}$$

To prepare chitosan solutions (10 μg/mL), chitosan was dissolved in a 150 mM acetic acid (pH 3.0) solution. Three buffers with different pHs were prepared: 150 mM acetic acid (pH 3.0), 150 mM sodium acetate buffer (pH 6.5), and 150 mM phosphate buffer (pH 8.5).

Preparation of Surface. Atomically smooth mica surfaces (Grade #1, S&J Trading, Inc.) were freshly cleaved under a laminar flow hood and were placed on another large freshly cleaved mica backing sheet. A silver layer (Cerac, purity > 99.99%) of uniform thickness (55 nm) was deposited using a Joule effect vapor deposition. Before chitosan deposition, the silvered mica sheets were glued (silver side down) on cylindrical glass disks using an epoxy glue (EPON 1004 F, Exxon Chemicals).[27,28]

Interaction Forces Measurement Using a Surface Forces Apparatus (SFA). The normal force−distance profiles and cohesion/adhesion forces of chitosan films were determined using a surface forces apparatus 2000 in a configuration that was previously reported in literature.[24,29] Chitosan was physically deposited on the back-silvered mica. The glued mica surface was dipped into a prepared chitosan solution (10 μg/mL in 150 mM acetic acid, pH 3.0) for 20 min followed by a thorough rinsing with the buffer solution (150 mM acetic acid, pH 3.0) in order to remove unbound chitosan. Depending on the experiment conducted, either two chitosan coated surfaces (symmetric) or one chitosan coated surface and one bare mica surface (asymmetric) were transferred into the SFA chamber in crossed-cylinder geometry which corresponds to a sphere of radius R approaching a flat surface on the basis of the Derjaguin approximation.[30] A droplet (50 μL) of buffer (pH 3.0) was injected between the transferred surfaces. The SFA chamber was sealed and was saturated with water vapor during the experiments. After mounting of the surfaces and injection of the buffer, the system was allowed to equilibrate for 1 h. All experiments were conducted at room temperature (T = 23 °C). The force (F) was measured by determining the deflection of the double cantilever spring (k = 3030 N/m) of the lower surface, and the distance (D) between two mica surfaces was measured from the fringes of equal chromatic order (FECO) using optical interferometry.[27] The lower surface was connected to a motor, which allows the two surfaces to move relative to each other at a controlled speed (∼3 nm/s in this study). R is the radius of the cylindrical silica disk (usually ∼2 cm), and D is the surface separation distance between two bare mica surfaces. The measured adhesion or normalized pull-off force F_{ad}/R ($= -\min[F/R]$) is related to the adhesion energy per unit area W_{ad} by $W_{ad} = 2F_{ad}/3\pi R$, the Johnson−Kendall−Roberts (JKR) model for soft materials with large deformations.[28,30] For calculating the surface energy during approach, which was always repulsive without flattening of the surfaces, the Derjaguin approximation, $W = F/2\pi R$, was used.[28,30] The surfaces were approached to contact (around $F/R \sim 4$ mN/m) and were kept in contact for durations of 5 s, 2 min, 10 min, and 1 h followed by separation to investigate the

effect of contact time on cohesion/adhesion forces of the chitosan films. Force versus distance profiles were measured multiple times at each condition to confirm their reproducibility. In addition to the force measurement under the pH 3.0 buffer, the measurements were repeated after replacing the buffer with an excess amount of 150 mM sodium acetate buffer solution (pH 6.5) and 150 mM phosphate buffer solution (pH 8.5) to study the effects of pH.

Atomic Force Microscopy (AFM). Freshly cleaved mica surfaces were dipped into a prepared chitosan solution (10 μg/mL in 150 mM acetic acid, pH 3.0) for 20 min followed by a thorough rinsing with the buffer solution (150 mM acetic acid, pH 3.0) in order to remove unbound chitosan. The chitosan film on mica surface was incubated for 1 h under three different pHs (3.0, 6.5, 8.5). Images were acquired using a Nanoscope III AFM (Veeco, Santa Barbara, CA, US) using a silicon nitride probe (Olympus, Tokyo, Japan) with a spring constant of 0.35 N m^{-1}. Scanning was performed in tapping mode at room temperature (22 ± 1 °C).

■ RESULTS AND DISCUSSION

Chitosan Adsorption on Mica. Adhesion and cohesion of chitosan can be influenced by the degree of deacetylation (DDA) of chitosan which modifies its crystalline structure. Therefore, the degree of acetylation (DA) of chitosan was estimated by ^{1}H NMR measurement prior to the SFA experiment. The DA of chitosan used in this study was ~19% (see Figure S1 of the Supporting Information). The interaction forces between two layers of chitosan adsorbed on mica surfaces or between chitosan film and mica were measured using an SFA. The adsorption of chitosan to mica was mainly driven by electrostatic attraction between positively charged chitosan molecules at pH 3.0 and negatively charged mica surfaces. The surfaces were thoroughly washed with 0.15 M acetic acid to remove unbound chitosan molecules before the SFA experiment. The adsorption of chitosan to mica was confirmed by the increase in the steric wall distance (D_{sw}, defined as the D at $F/R \sim 4$ mN/m). The thickness of chitosan films, as measured by D_{sw}, was ~1.5 nm per surface, which is similar to values reported by a previous study.[19] Although a comprehensive configuration of chitosan film on mica is difficult to resolve experimentally, D_{sw} from the SFA experiments can give some clues to deduce the configuration of chitosan film on mica. The measured contour length of chitosan used in this study was around 1000 nm,[31] and the radius of gyration of chitosan (R_g) expected by the empirical equation,[32] $R_g = 0.075 \cdot (MW)^{0.55}$, is ~50 nm in an acidic environment. The R_g of chitosan with a similar molecular weight in acidic buffer determined by dynamic light scattering was also ~50 nm.[33]

The repulsive force started around $D > 20$ nm on approach (Figure 2A) with a decay length of ~7 nm, indicating a swollen structure (exposing loops) of initially adsorbed chitosan. The measured decay length on approach might be related to the thickness of loops of initial chitosan structure. After the compression (up to $F/R \sim 4$ mN/m), the film thickness as measured by D_{sw} of one chitosan film (~1.5 nm) at pH 3.0 was much less than the expected radius of gyration of 50 nm.[32,33] Consequently, these measurements indicate that chitosan would be in a flat conformation under confinement.[34] Also, there was no observed hysteresis on approach possibly because of rapid changes to the initial swollen structure on separation
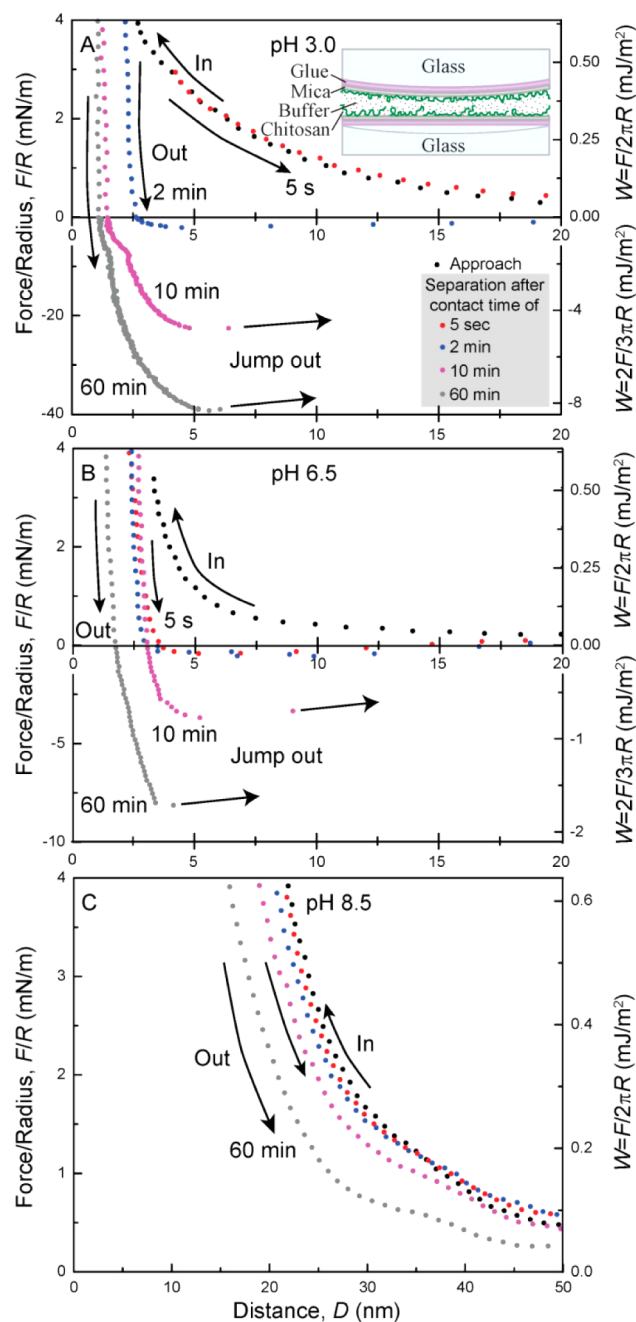

Figure 2. Force profiles between two physisorbed chitosan surfaces in (A) pH 3.0 and 150 mM acetic acid solution, (B) pH 6.5 and 150 mM sodium acetate buffer solution, and (C) pH 8.5 and 150 mM phosphate buffer solution with the contact times of 5 s, 2 min, 10 min, and 1 h. All force curves are the representative results at each experiment condition.

by pulling out the looped residues of chitosan molecules from adhesive contact.

Cohesion of Chitosan Films (Symmetric Configuration). *Contact Time Effect.* At pH 3.0, normalized cohesion forces between the two chitosan films, F_{co}/R (= −min[F/R]), on the separation depended mostly on the contact time, t_{ct} (Figure 2A). No cohesion was initially measured between two chitosan films at $t_{ct} \sim 5$ s, and the surfaces were purely repulsive with steric wall, D_{sw}, of ~3 nm. However, as t_{ct} increased from 2 min to 1 h, the following results were observed: (1) the repulsion disappeared and F_{co}/R increased from ~2 to ~40
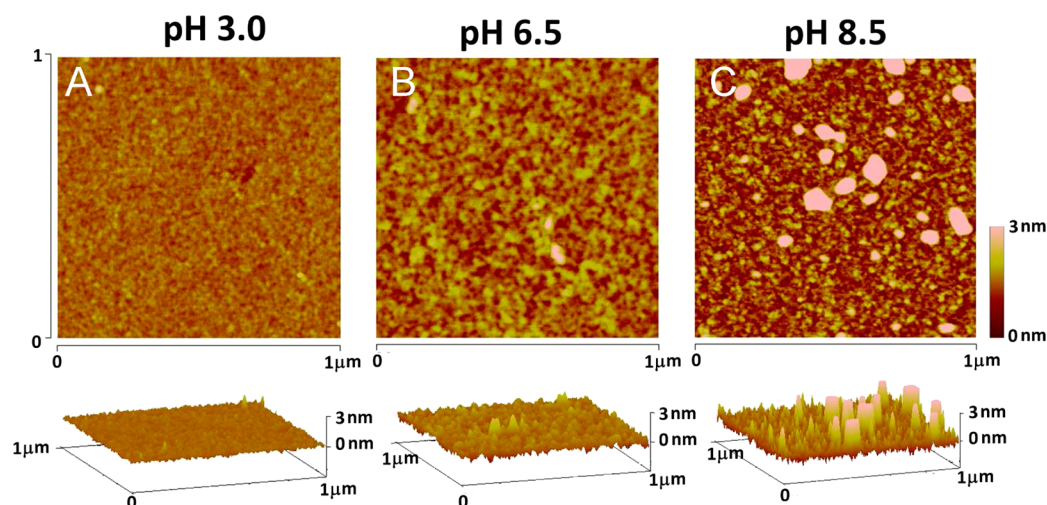
Figure 3. AFM tapping mode images of chitosan films on freshly cleaved mica deposited at pH 3.0 and incubated for 1 h at pH (A) 3.0, (B) 6.5, and (C) 8.5.

mN/m, and the right-hand y-axis shows that these forces correspond to surface cohesion energies of W_{co} from $\sim$0.4 to $\sim$8.5 mJ/m^2. (2) D_{sw} decreased from $\sim$3 nm to $\sim$1 nm. (3) Repeated contact and separation with 5 s of t_{ct} after breaking the 1 h contact produced a W_{co} of $\sim$0.85 mJ/m^2. Previous studies with chitosan films only showed a relatively weak cohesion force of $\sim$0.5 mN/m ($W_{co} \sim$ 0.1 mJ/m^2) at pH 3.8 with 2 mM of acetic acid, which is probably due to relatively short contact time.[19] The cohesive energy W_{co} of $\sim$8.5 mJ/m^2 measured in the present study is about 60% of the interaction between the strongest, previously reported, mussel adhesive protein to mica (Mefp-5 to mica, $W_{ad} \sim$ 14 mJ/m^2).[35]

Effects of pH on Cohesion of Chitosan. Figure 2 shows the interaction forces between two chitosan physisorbed surfaces (symmetric configuration, see the schematic in Figure 2A) in 0.15 M buffer solutions at three pHs (3.0, 6.5, and 8.5). As the previously reported pK_a value of chitosan is around 6.5−7.0, we chose pH 3.0 as most glucosamine units in chitosan would be protonated, pH 6.5 as half of the glucosamine would be protonated, and pH 8.5 as most glucosamine would not be protonated. The cohesion energy, W_{co}, of chitosan films decreased with increasing pH from $\sim$8.5 mJ/m^2 at pH 3.0 to $\sim$1.7 mJ/m^2 at pH 6.5 and to 0 mJ/m^2 at pH 8.5. On the other hand, D_{sw} increased with increasing pH from $\sim$2.5 nm at pH 3.0 to $\sim$3 nm at pH 6.5 and to $\sim$24 nm at pH 8.5. These results are consistent with the previous work done by Claesson and Ninham[19] which also showed a decrease in adhesion force and an increase in the chitosan layer thickness with an increase in pH. To confirm that the chitosan thickness increased while increasing the buffer pH, we prepared equivalent adsorbed chitosan surfaces on mica. The root-mean-square (RMS) surface roughness determined by atomic force microscopy (AFM) for surfaces at pH 3.0, 6.5, and 8.5 were 0.14, 0.30, and 0.96 nm, respectively (see Figure 3). AFM topology of the chitosan film on mica showed that chitosan layers were roughened by increasing the solution pH as observed in the SFA. Because the adhesion between two elastic surfaces is generally reduced with increasing the surface roughness,[36] the lack of adhesion between two opposing chitosan surfaces at pH 8.5 was also influenced by the surface roughness.

Proposed Mechanism for Cohesion of Two Opposed Chitosan Layers. It was previously demonstrated using the SFA

that the thickness of adsorbed chitosan on mica was not increased even after 24 h of incubation with 0.01% (w/v) acetic acid containing 0.01% (w/v) chitosan. This suggested that chitosan molecules initially might not have cohesion in acetic acid solutions.[19] Consistent with the previous study, two opposed positively charged chitosan films did not have any cohesive interaction in acetate buffers with a short contact time. However, with an increase in the contact time, cohesion between the chitosan layers began to occur. Additionally, higher contact times resulted in higher cohesive energy and lower D_{sw} between two opposing chitosan films. These observations are typical signs of molecular rearrangement and cohesive bond (cohesive/adhesive bonds indicated in this study include physical bonds induced by all types of attractive interactions such as electrostatic, hydrophobic, and van der Waals) formation while the surfaces are in contact. The increase in cohesion with time was probably due to a rearrangement of chitosan molecules into an orientation proper for cohesion while in contact with the opposing surface, resulting in stronger cohesive interaction over time. Indeed, conformational transitions of chitosan molecules have been reported to occur as the local environment around the chitosan molecule changes (pH, temperature, and types of acid and salts).[15] Up to now, four types of X-ray crystal structures of chitosan (extended 2-fold helix, relaxed 2-fold helix, 4/1 helix, and 5/3 helix) have been identified, each depending on the local environment. Because 4/1 helix and 5/3 helix only occur in the presence of iodide ions and aromatic organic acids, respectively, these helixes are not likely to be formed in the present study.[12,13] It is reported that chitosan prefers to take up a relaxed 2-fold helix structure which does not form strong intramolecular hydrogen bonds in acetate buffer systems[16,18] similar to what we used in our SFA experiments. Therefore, chitosan molecules adsorbed on mica would initially exhibit a relaxed 2-fold helix with higher thickness (see Summary and Conclusion). On the basis of the D_{sw} reduction with the increase of t_{ct} (from 3 to 1 nm), chitosan molecules adsorbed to mica presumably changed to an extended 2-fold helix, which is a zigzag structure similar to that of chitin and cellulose.[16,18] The contact time effects imply that strong cohesion may arise from a conformational change from a relaxed 2-fold helix to an extended 2-fold helix caused by confinement of chitosan chains at the contact. Consequently,

the structural change is enhanced at pH 3.0 because of the flexibility of the chitosan chains[37−39] that promotes their rearrangement to form hydrogen bonds and hydrophobic interactions against chitosan at the opposing surface (see Figure 1 for hydrogen-bonding sites). Furthermore, on the basis of the DA measurement, chitosan used in this study was composed of 19 mol % of N-acetyl-D-glucosamine and 81 mol % of D-glucosamine. Relatively hydrophobic methyl groups in the N-acetyl-D-glucosamine unit would be initially hidden because of long incubation with aqueous buffer, but it could be exposed to the methyl group of N-acetyl-D-glucosamine on the other surface, resulting in increases in adhesion because of hydrophobic interactions. Both hydrogen bonds and hydrophobic interactions of the methyl groups are likely to be responsible for the exceptionally high cohesion force between the chitosan physisorbed surfaces. Successive force measurements (t_{ct} = 5 s) right after the force run with t_{ct} of 1 h were quite reproducible, implying that proper orientation for strong cohesion can be maintained for a certain amount of time.

Besides the rearrangement and structural change of chitosan chains, ion diffusion/migration and charge regulation established at the contact could be a factor in decreasing electrostatic repulsion which, in turn, increases the adhesion force. The charge regulation can affect the interaction forces between chitosan surfaces, but the adhesion forces due to hydrogen bonding and hydrophobic attraction are dominant. Also, in this system with a high anion concentration (15−150 mM), charge regulation will occur in a very short time; thus, chitosan rearrangement will likely to be the rate-limiting step.

At pH 6.5, amine groups in chitosan are less protonated compared to pH 3.0, causing the chitosan chains to be less flexible.[40] Accordingly, D_{sw} is thicker and F_{co} is significantly smaller (∼1.6 mJ/m² at t_{ct} = 1 h) compared to pH 3.0 (see Figure 2B). In other words, it takes more time for chitosan chains to change their conformation. At pH 8.5, most of the amine groups are not protonated and the solubility of chitosan decreases drastically, making chitosan layers extremely rigid and immobile. As a result, D_{sw} significantly thickens (∼23 nm), and the force profiles between chitosan physisorbed surfaces become purely repulsive because of steric repulsion (see Figure 2C) which overwhelms all other attractive interaction forces. Also, at this pH, chitosan chains are too rigid to rearrange and form hydrogen bonds or to exhibit noticeable hydrophobic attraction in a short time (t_{ct} < 1 h).

Chitosan Adhesion to Mica (Asymmetric Configuration). *Effect of Contact Time and pH.* Figure 4 shows the interaction forces between chitosan physisorbed surfaces and mica (see the schematic in Figure 4A). The same experimental conditions (pH and t_{ct}) are applied as the symmetric case (Figure 2) in order to see the normalized adhesion force, F_{ad}/R (= −min[F/R]), of chitosan layer to mica. In contrast to the symmetric configuration, a strong adhesion F_{ad}/R ∼ 18 mN/m (W_{ad} ∼ 3.8 mJ/m²) was observed at pH 3.0 with only a 5 s contact. The thickness of one chitosan layer measured by D_{sw} was similar to the symmetric configuration (∼1.5 nm). When the chitosan film stayed in contact with mica, W_{ad} reached a plateau at the 10 min contact time (Figure 4A). The adhesion significantly decreased with increasing buffer pH from W_{ad} ∼ 3.8 mJ/m² at pH 3.0 to W_{ad} ∼ 0.6 mJ/m² at pH 6.5 and to W_{ad} ∼ 0.4 mJ/m² at pH 8.5 (Figure 4B and C). On the other hand, W_{ad} did not plateau at higher pH unlike pH 3.0 and was still increasing with increasing contact time (Figure 5B). The decrease of the adhesion of chitosan film to mica with
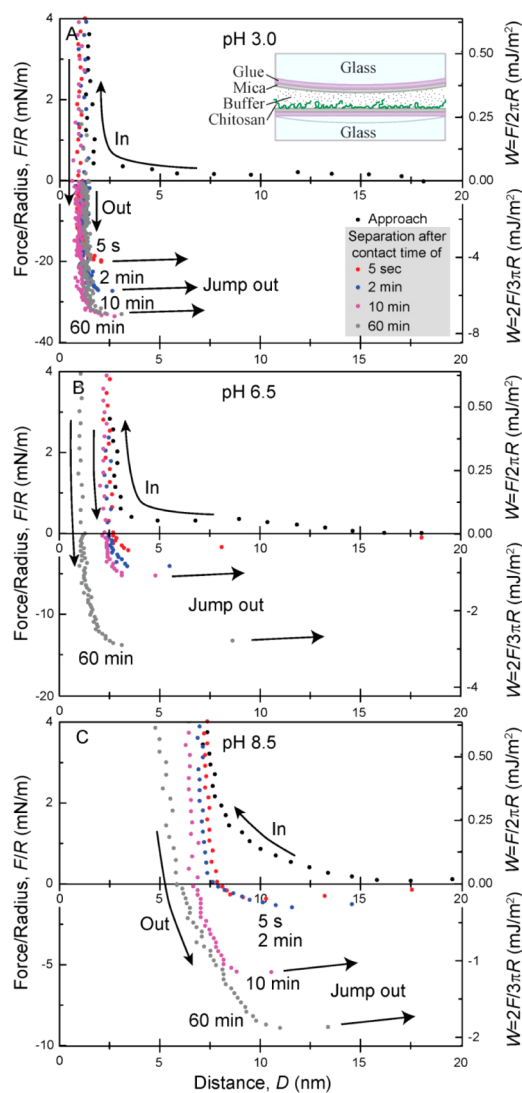

Figure 4. Force profiles between physisorbed chitosan surfaces against mica in (A) pH 3.0 and 150 mM acetic acid solution, (B) pH 6.5 and 150 mM sodium acetate buffer solution, and (C) pH 8.5 and 150 mM phosphate buffer solution with the contact times of 5 s, 2 min, 10 min, and 1 h. All force curves are the representative results at each experiment condition.

increasing pH is likely to be related to the reduction of the positively charged D-glucosamine unit in chitosan because it has a pK_a of 6.5−7.0. Similar to symmetric cases, D_{sw} decreased with an increase in contact time and increased with an increase in pH. The results show that the D_{sw} decrease and the F_{ad}/R increase with the increase in t_{ct} are similar to symmetric cases. However, the following discrepancies are observed compared to symmetric cases: (1) repulsion is smaller on approach, (2) D_{sw} is smaller (up to ∼50%), (3) at pH 8.5, surfaces are adhesive, and (4) at pH 3.0, repeated contact and separation with 5 s of t_{ct} after breaking the 1 h contact produced a W_{ad} ∼ 5.1 mJ/m², which is a rather small increase from ∼3.8 mJ/m². These differences are expected because the chitosan is only physisorbed to one surface and opposing surfaces are now under electrostatic attraction at pH 3.0 and 6.5 (negative mica and positive chitosan film). Meanwhile, at pH 8.5, even though most of the amines in chitosan are not protonated and electrostatic attraction is eliminated, the surfaces remain
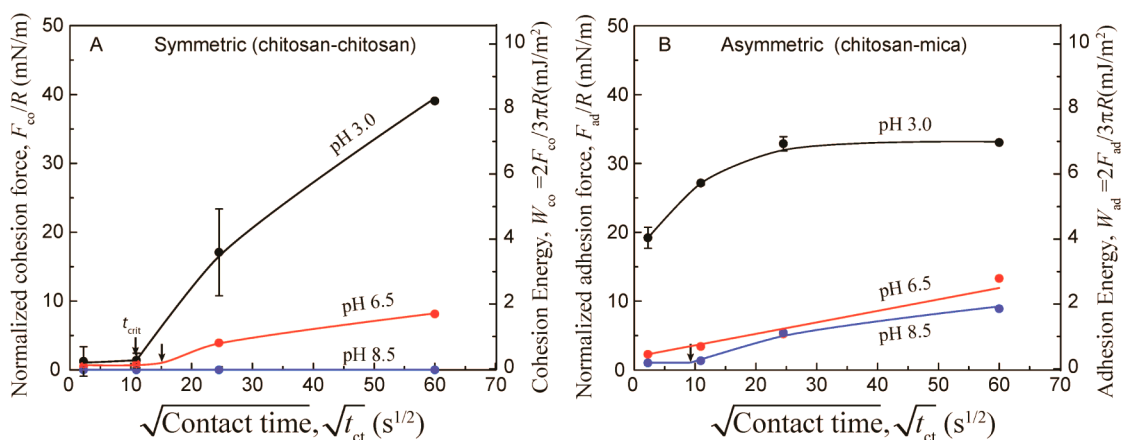
Figure 5. Normalized cohesion/adhesion force (energy) vs contact time curve for symmetric (chitosan vs chitosan) and asymmetric (chitosan vs mica) cases under the applied load of ~4 mN/m at pHs of 3.0 (black), 6.5 (red), and 8.5 (blue). Arrows indicate critical contact time, t_{crit}, where surfaces become adhesive.
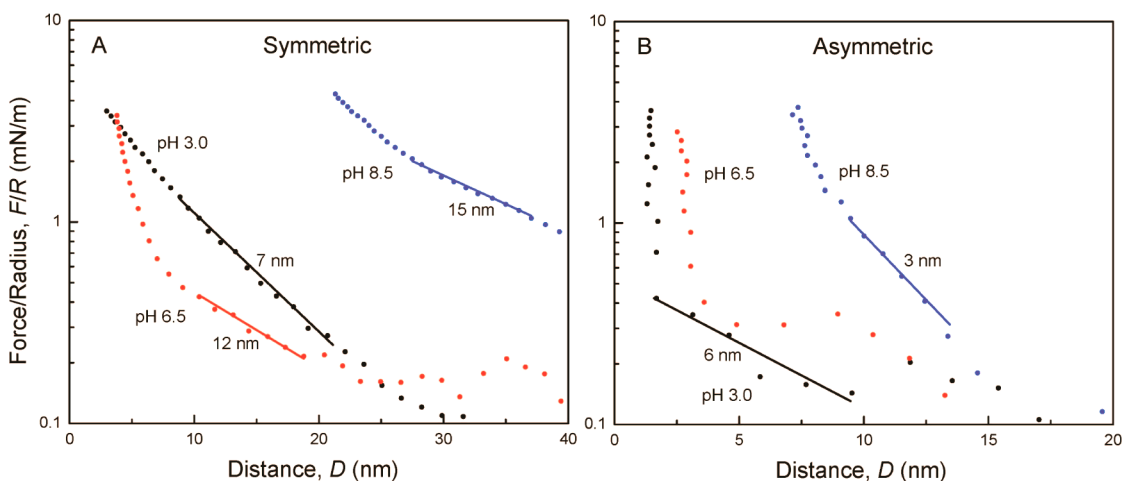
Figure 6. Approach curves for symmetric and asymmetric cases at pHs of 3.0, 6.5, and 8.5. The calculated Debye lengths were ~2.5, ~0.8, and ~0.8 nm, respectively. The larger decay lengths compared to the Debye lengths indicate that steric contribution is significant on approach for all cases.

adhesive. This is due to the rapid formation of hydrogen bonds and van der Waals forces between mica and chitosan.

Contact Time Effects on the Cohesion/Adhesion Forces. The rate of cohesive/adhesive bond formation depends both on the time needed to overcome electrostatic/steric repulsion (activation energy) and on the mobility of chitosan chains for hydrogen donors to find hydrogen acceptors at opposing surfaces. These repulsions induce a critical time,[41,42] t_{crit}, before chitosan changes structure and starts forming hydrogen bonds. t_{crit} highly depends on pH because increasing pH not only makes the chitosan chains neutral but also decreases the solubility and makes the chains rigid and immobile.

Figure 5 shows the time evolution of the cohesion and adhesion forces which reveals important clues to understanding the system. In the case of the symmetric surfaces (Figure 5A) at pHs 3.0 and 6.5, the chitosan chains are fully and half protonated, respectively, and cause the surfaces to repel on approach. Moreover, the measured decay lengths are larger than the Debye lengths (see Figure 6) indicating that steric repulsions between opposing chitosan chains are also significant. At pH 8.5, electrostatic repulsion is eliminated because of the deprotonation of the chitosan chains, but the higher rigidity induces even higher repulsion. The increase of

t_{crit} with pH also indicates that the chitosan chains become more rigid and less mobile. For the symmetric case (Figure 5A), t_{crit} was ~120 s at pH 3.0, it was ~220 s at pH 6.5, and at pH 8.5, it was too high to be measured (t_{crit} > 1 h).

Meanwhile, at pHs 3.0 and 6.5, chitosan and mica surfaces (Figure 5B) are electrostatically attractive. As a result, for pHs 3.0 and 6.5, t_{crit} was too small to be measured (<5 s), and for pH 8.5, t_{crit} was ~100 s. These results indicate that the time for chitosan to form an adhesive bond with mica was much faster than the chitosan surface forming cohesive bonds. For both the symmetric and the asymmetric cases, when t_{ct} > t_{crit}, F_{co} and F_{ad} scaled as ~$t_{ct}^{1/2}$, which suggests that they are diffusion-controlled processes, as previously reported.[43,44] In this regime, chitosan molecules are adjusting their position and orientation by diffusion to form a conformation which can maximize the adhesion energy. As t_{ct} increases further, the adhesion and cohesion forces plateau to certain values as the rate of adhesive bond formation approaches zero.[41] This saturation was observed at pH 3.0 for the asymmetric case at t_{ct} ~ 400 s. However, for the symmetric case, no complete saturation was observed even for 1 h of contact time, indicating that the saturation occurs at t_{ct} > 1 h.
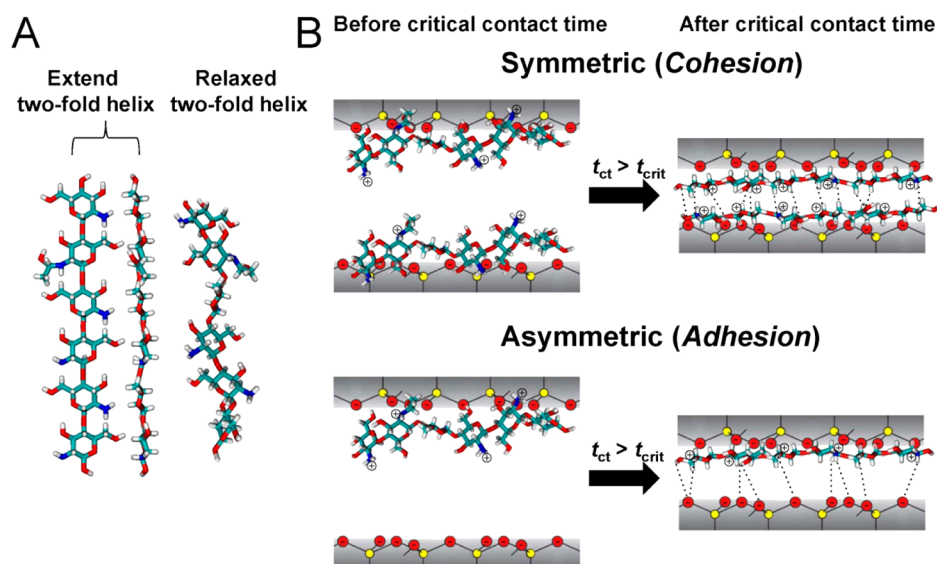
Figure 7. (A) Molecular structure of chitosan (left and center) extended 2-fold helix[17] and (right) relaxed 2-fold helix[13] as determined by X-ray crystallography. (B) Schematic representation of the putative cohesion (top right, chitosan vs chitosan) and adhesion (bottom right, chitosan vs mica) mechanisms of chitosan film in wet conditions. Atoms color coded as cyan, carbon; red, oxygen; blue, nitrogeon; white, hydrogen; yellow, silicon. Putative hydrogen bonds are shown as dotted lines.

■ SUMMARY AND CONCLUSION

The proposed chitosan interaction mechanisms are shown schematically in Figure 7. On the basis of the SFA results and discussions above, the interaction mechanisms between two opposed chitosan films (symmetric configuration) and between a chitosan film and mica (asymmetric configuration) can be summarized as follows:

(1) For the symmetric configuration (chitosan vs chitosan cohesion), the critical contact time to achieve cohesion between two chitosan films was relatively long, and the cohesive energy between the chitosan films at pH 3.0 was strong ($W_{ad} \sim 8.5$ mJ/m^2), reaching nearly 60% of the strongest mussel adhesive protein (mefp-5) to mica. Here, we speculate that the contact time dependence of the self-interactions of chitosan molecules is probably related to the formation of hydrogen bonds enhanced by structural changes in the chitosan molecules from a relaxed 2-fold helix (a chitosan structure in dilute acetic acid) to an extended 2-fold helix (a chitosan structure with zigzag structure which is similar to those of chitin and cellulose) because of the confinement of the chitosan films during contact.

(2) For the asymmetric configuration (chitosan vs mica adhesion), chitosan strongly interacted with a negatively charged mica surface via electrostatic forces when the chitosan molecule was positively charged. However, it can also interact with the mica via other interaction forces such as hydrogen bonds and van der Waals forces between the D-glucosamine units in chitosan and hydrated mica surfaces.

In conclusion, we directly measured the strong molecular interactions of chitosan using an SFA; these measurements provided insights into the self-assembly of chitosan molecules in wet conditions. Our SFA study showed strong adhesive interactions between chitosan and mica and strong cohesive strength between two opposed chitosan films in acidic buffer. The chitosan interactions decreased with increasing buffer pH,

which is proposed to be mainly due to the reduction in solubility of chitosan molecules as they are not protonated at higher pH. Our results should be applicable to the use of chitosan in various biomedical applications.

■ ASSOCIATED CONTENT

Ⓢ Supporting Information
Degree of deacetylation of chitosan molecule used in this study by ^{1}H NMR measurement. This material is available free of charge via the Internet at http://pubs.acs.org.

■ AUTHOR INFORMATION

Corresponding Authors
*E-mail: Jacob@engineering.ucsb.edu. Phone: (805) 893-8407. Fax: (805) 893-7870.
*E-mail: dshwang@postech.ac.kr. Phone: +82(54) 279-9505. Fax: +82(54) 279-9519.
Notes
The authors declare no competing financial interest.

■ ACKNOWLEDGMENTS

■ REFERENCES

(1) Cunha, R. A.; Soares, T. A.; Rusu, V. H.; Pontes, F. J. S.; Franca, E. F.; Lins, R. D. The Molecular Structure and Conformational Dynamics of Chitosan Polymers: An Integrated Perspective from Experiments and Computational Simulations. In *The Complex World of Polysaccharides*; Karunaratne, D. N., Ed.; Intech: Rijeka, Croatia, 2012.

(2) Ifuku, S.; Nogi, M.; Abe, K.; Yoshioka, M.; Morimoto, M.; Saimoto, H.; Yano, H. Preparation of chitin nanofibers with a uniform width as alpha-chitin from crab shells. *Biomacromolecules* **2009**, *10* (6), 1584−1588.

(3) Kurita, K. Chitin and chitosan: Functional biopolymers from marine crustaceans. *Mar. Biotechnol.* **2006**, *8* (3), 203−226.

(4) Kumar, M. A review of chitin and chitosan applications. *React. Funct. Polym.* **2000**, *46* (1), 1−27.

(5) Chang, K. L. B.; Tsai, G.; Lee, J.; Fu, W. R. Heterogeneous N-deacetylation of chitin in alkaline solution. *Carbohydr. Res.* **1997**, *303* (3), 327−332.

(6) Wang, W. P.; Du, Y. M.; Qiu, Y. L.; Wang, X. Y.; Hu, Y.; Yang, J. H.; Cai, J.; Kennedy, J. F. A new green technology for direct production of low molecular weight chitosan. *Carbohydr. Polym.* **2008**, *74* (1), 127−132.

(7) Wei, Z. J.; Wang, C. Y.; Zou, S. W.; Liu, H.; Tong, Z. Chitosan nanoparticles as particular emulsifier for preparation of novel pH-responsive Pickering emulsions and PLGA microcapsules. *Polymer* **2012**, *53* (6), 1229−1235.

(8) Riccardo, A. A.; Uzzarelli, M.; Isolati, A. Methyl mercury acetate removal from waters by chromatography on chelating polymers. *Water, Air, Soil Pollut.* **1971**, *1*, 65−71.

(9) Yi, H. M.; Wu, L. Q.; Bentley, W. E.; Ghodssi, R.; Rubloff, G. W.; Culver, J. N.; Payne, G. F. Biofabrication with chitosan. *Biomacromolecules* **2005**, *6* (6), 2881−2894.

(10) Kumar, M. N. V. R.; Muzzarelli, R. A. A.; Muzzarelli, C.; Sashiwa, H.; Domb, A. J. Chitosan chemistry and pharmaceutical perspectives. *Chem. Rev.* **2004**, *104* (12), 6017−6084.

(11) Ogawa, K.; Inukai, S. X-Ray diffraction study of sulfuric, nitric, and halogen acid salts of chitosan. *Carbohydr. Res.* **1987**, *160*, 425−433.

(12) Kawahara, M.; Yui, T.; Oka, K.; Zugenmaier, P.; Suzuki, S.; Kitamura, S.; Okuyama, K.; Ogawa, K. Fourth 3D structure of the chitosan molecule: Conformation of chitosan in its salts with medical organic acids having a phenyl group. *Biosci., Biotechnol., Biochem.* **2003**, *67* (7), 1545−1550.

(13) Lertworasirikul, A.; Tsue, S.; Noguchi, K.; Okuyama, K.; Ogawa, K. Two different molecular conformations found in chitosan type II salts. *Carbohydr. Res.* **2003**, *338* (11), 1229−1233.

(14) Ogawa, K. Effect of heating an aqueous suspension of chitosan on the crystallinity and polymorphs. *Agric. Biol. Chem.* **1991**, *55*, 2375−2379.

(15) Ogawa, K.; Yui, T.; Okuyama, K. Three D structures of chitosan. *Int. J. Biol. Macromol.* **2004**, *34* (1−2), 1−8.

(16) Okuyama, K.; Noguchi, K.; Kanenari, M.; Egawa, T.; Osawa, K.; Ogawa, K. Structural diversity of chitosan and its complexes. *Carbohydr. Polym.* **2000**, *41* (3), 237−247.

(17) Okuyama, K.; Noguchi, K.; Miyazawa, T.; Yui, T.; Ogawa, K. Molecular and crystal structure of hydrated chitosan. *Macromolecules* **1997**, *30* (19), 5849−5855.

(18) Okuyama, K.; Osawa, K.; Hanafusa, Y.; Noguchi, K.; Ogawa, K. Relaxed 2/1-helical conformation of type II chitosan has a tetrasaccharide motif. *J. Carbohydr. Chem.* **2000**, *19* (6), 789−794.

(19) Claesson, P. M.; Ninham, B. W. PH-dependent interactions between adsorbed chitosan layers. *Langmuir* **1992**, *8* (5), 1406−1412.

(20) Greene, G. W.; Banquy, X.; Lee, D. W.; Lowrey, D. D.; Yu, J.; Israelachvili, J. N. Adaptive mechanically controlled lubrication mechanism found in articular joints. *Proc. Natl. Acad. Sci. U.S.A.* **2011**, *108* (13), 5255−5259.

(21) Lee, D. W.; Banquy, X.; Israelachvili, J. N. Stick-slip friction and wear of articular joints. *Proc. Natl. Acad. Sci. U.S.A.* **2013**, *110* (7), E567−E574.

(22) Lu, Q. Y.; Danner, E.; Waite, J. H.; Israelachvili, J. N.; Zeng, H. B.; Hwang, D. S. Adhesion of mussel foot proteins to different substrate surfaces. *J. R. Soc., Interface* **2013**, *10* (79), 11.

(23) Sivasankar, S.; Brieher, W.; Lavrik, N.; Gumbiner, B.; Leckband, D. Direct molecular force measurements of multiple adhesive interactions between cadherin ectodomains. *Proc. Natl. Acad. Sci. U.S.A.* **1999**, *96* (21), 11820−11824.

(24) Israelachvili, J.; Min, Y.; Akbulut, M.; Alig, A.; Carver, G.; Greene, W.; Kristiansen, K.; Meyer, E.; Pesika, N.; Rosenberg, K.; Zeng, H. Recent advances in the surface forces apparatus (SFA) technique. *Rep. Prog. Phys.* **2010**, *73* (3), 16.

(25) Hwang, D. S.; Zeng, H. B.; Lu, Q. Y.; Israelachvili, J.; Waite, J. H. Adhesion mechanism in a DOPA-deficient foot protein from green mussels. *Soft Matter* **2012**, *8* (20), 5640−5648.

(26) Hirai, A.; Odani, H.; Nakajima, A. Determination of degree of deacetylation of chitosan by 1H NMR spectroscopy. *Polym. Bull.* **1991**, *26*, 87−94.

(27) Israelachvili, J. Thin-film studies using multiple-beam interferometry. *J. Colloid Interface Sci.* **1973**, *44* (2), 259−272.

(28) Israelachvili, J. N. *Intermolecular and Surface Forces*, 3rd ed.; Academic Press and Elsevier: Amsterdam, 2011.

(29) Hwang, D. S.; Zeng, H. B.; Masic, A.; Harrington, M. J.; Israelachvili, J. N.; Waite, J. H. Protein- and metal-dependent interactions of a prominent protein in mussel adhesive plaques. *J. Biol. Chem.* **2010**, *285* (33), 25850−25858.

(30) Johnson, K. L.; Kendall, K.; Roberts, A. D. Surface energy and contact of elastic solids. *Proc. R. Soc. London, Ser. A: Math. Phys. Sci.* **1971**, *324* (1558), 301−313.

(31) Hu, Y.; Wu, Y. Z.; Cai, J. Y.; Ma, Y. F.; Wang, B.; Xia, K.; He, X. Q. Self-assembly and fractal feature of chitosan and its conjugate with metal ions: Cu(II)/Ag(I). *Int. J. Mol. Sci.* **2007**, *8* (1), 1−12.

(32) Rinaudo, M. Chitin and chitosan: Properties and applications. *Prog. Polym. Sci.* **2006**, *31* (7), 603−632.

(33) Wu, C.; Zhou, S. Q.; Wang, W. A dynamic laser light-scattering study of chitosan in aqueous-solution. *Biopolymers* **1995**, *35* (4), 385−392.

(34) Lescanec, R. L.; Muthukumar, M. Configurational characteristics and scaling behavior of starburst molecules: a computational study. *Macromolecules* **1990**, *23*, 2280−2288.

(35) Danner, E. W.; Kan, Y. J.; Hammer, M. U.; Israelachvili, J. N.; Waite, J. H. Adhesion of mussel foot protein Mefp-5 to mica: An underwater superglue. *Biochemistry* **2012**, *51* (33), 6511−6518.

(36) Fuller, K. N. G.; Tabor, D. Effect of surface-roughness on adhesion of elastic solids. *Proc. R. Soc. London, Ser. A: Math. Phys. Eng. Sci.* **1975**, *345* (1642), 327−342.

(37) Franca, E. F.; Freitas, L. C. G.; Lins, R. D. Chitosan molecular structure as a function of N-acetylation. *Biopolymers* **2011**, *95* (7), 448−460.

(38) Franca, E. F.; Lins, R. D.; Freitas, L. C. G.; Straatsma, T. P. Characterization of chitin and chitosan molecular structure in aqueous solution. *J. Chem. Theory Comput.* **2008**, *4* (12), 2141−2149.

(39) Skovstrup, S.; Hansen, S. G.; Skrydstrup, T.; Schiott, B. Conformational flexibility of chitosan: A molecular modeling study. *Biomacromolecules* **2010**, *11* (11), 3196−3207.

(40) Chen, R. H.; Tsaih, M. L.; Lin, W. C. Effects of chain flexibility of chitosan molecules on the preparation, physical, and release characteristics of the prepared capsule. *Carbohydr. Polym.* **1996**, *31* (3), 141−148.

(41) Xu, L. C.; Siedlecki, C. A. Effects of surface wettability and contact time on protein adhesion to biomaterial surfaces. *Biomaterials* **2007**, *28* (22), 3273−3283.

(42) Xu, L. C.; Vadillo-Rodriguez, V.; Logan, B. E. Residence time, loading force, pH, and ionic strength affect adhesion forces between colloids and biopolymer-coated surfaces. *Langmuir* **2005**, *21* (16), 7491−7500.

(43) Banquy, X.; Kristiansen, K.; Lee, D. W.; Israelachvili, J. N. Adhesion and hemifusion of cytoplasmic myelin lipid membranes are highly dependent on the lipid composition. *Biochim. Biophys. Acta: Biomembr.* **2012**, *1818* (3), 402−410.

(44) Meyer, E. E.; Rosenberg, K. J.; Israelachvili, J. Recent progress in understanding hydrophobic interactions. *Proc. Natl. Acad. Sci. U.S.A.* **2006**, *103* (43), 15739−15746.